

# Geothermal Study Over Sokoto Basin Northwestern, Nigeria

Kamureyina Ezekiel

Department Of Geology And Mining, Adamawa State University, Mubi P.M.B 25, Mubi, Nigeria

---

**Abstract:** The study was carried out to determine Curie point depth, geothermal gradient and heat flow using high resolution aeromagnetic data over the Sokoto basin. The quest for the study was necessitated as a result of the over dependence on the oil sector and hence the need to explore other earth endowments. This was achieved using statistical methods. The composite total magnetic intensity map was subjected to regional-residual separation using the polynomial fitting technique on the aeromagnetic data to obtain the residual data. The residual data was upward continued to 27km. The upward filtered data was fast Fourier transformed to obtain the radially average power spectrum after dividing the area into 64 blocks for spectral analysis to determine depth to the centroid and depth to the top boundary which was used to calculate Curie point depth, geothermal gradient and heat flow. The result of the analysis revealed that Curie Point Depth varies from 17.31km to 26.76km; Geothermal Gradient, 21.67 °Ckm<sup>-1</sup> to 33.50 °Ckm<sup>-1</sup> and Heat Flow, 54.18mWm<sup>-2</sup> to 83.64mWm<sup>-2</sup>. The investigation shows that the crust is thinning in areas of shallow Curie depth of 17.31km to 18.16km based on the Curie point isotherm deduced from the study; low geothermal gradient zones could not allow thermal maturation of the sediments, high geothermal gradient zones could result into thermal maturation of sediments and hence probable oil generation and the high heat flow of 80mWm<sup>-2</sup> and above are potentials areas for geothermal energy.

**Keywords:** Geothermal study; Aeromagnetic data; Curie point depth; Geothermal gradient; Heat flow; Geothermal energy; Sokoto; Nigeria.

---

Date of Submission: 25-04-2019

Date of acceptance: 05-05-2019

---

## I. Introduction

The study was carried out to determine Curie Point Depth, Geothermal gradient and Heat flow of the Sokoto basin, using high resolution digital aeromagnetic data. The data processing was achieved, through polynomial fitting, upward continuation and spectral analysis to calculate depth to centroid and depth to the top boundary and hence the estimation of the curie isotherm, geothermal gradient and heat flow.

The quest for search of geothermal energy have been necessitated as a result of the over dependence on oil sector, neglecting other earth endowments. This has adverse effect on the country in terms of fall in oil prices. Diversifying the economy to other sectors such as the geothermal energy and mineral resources will increase the economic growth and hence better living for the citizenry. The work will serve as a guide for detailed geophysical surveys for economic prospects and better understanding of the geology of the area in terms of sites for geothermal plants, which could be used for generation of electricity, domestic, industrial and agricultural purposes.

The findings of this study revealed that, Curie Point Depth varies from 17.31km to 26.76km; Geothermal Gradient, 21.67 °Ckm<sup>-1</sup> to 33.50 °Ckm<sup>-1</sup> and Heat Flow, 54.18mWm<sup>-2</sup> to 83.64mWm<sup>-2</sup>. These results are useful in understanding the variation in crustal thickness, thermal maturation of sediments and sites for geothermal energy.

Geophysical surveys are directed at obtaining indirectly, from the surface or from shallow depth, the physical parameters of the geothermal systems. A geothermal system is made up of four main elements: a heat source, a reservoir, a fluid, which is the carrier that transfers the heat, and a recharge area. The heat source is generally a shallow magmatic body, usually cooling and often still partially molten. The volume of rocks from which heat can be extracted is called the geothermal reservoir, which contains hot fluids, a summary term describing hot water, vapour and gases. A geothermal reservoir is usually surrounded by colder rocks that are hydraulically connected with the reservoir. Hence water may move from colder rocks outside the reservoir (recharge) towards the reservoir, where hot fluids move under the influence of buoyancy forces towards a discharge area. Geothermal systems exist in regions of high crustal heat flux that may be associated with the occurrence of young igneous bodies or hot rocks located deeper in the crust (Salem et al., 2000; DiPippio, 2005 and Blackwell et al., 2006).

The study area lies between longitudes 4°00'E and 6°00'E and latitudes 11°30'N and 13°30'N (Fig. 1) and covers an area of approximately 48400 km<sup>2</sup>. It is part of the Illumedden Basin of West Africa, locally known as the Sokoto embayment situated in northwestern Nigeria (Kogbe, 1976 and Affordile, 2002). It

consists predominantly of a gently undulating plain with an average elevation varying from 250 to 400m above sea level. The plain is occasionally interrupted by low Mesas. A low Escarpment known as the “Dange Scarp” is the most prominent feature in the basin. The area to the east of the escarpment consists of mainly an undulating sandy plain, which extends south-westwards to the outcropping basement complex (Affordile, 2002).

The Sokoto basin falls within the hottest parts of Nigeria, belonging to the Sahel region of Africa. Temperatures are generally extreme, with average daily minimum of 16°C, during cool months of January and December, and the hottest months of April to June with an average maximum of 38°C and minimum of 24°C. Throughout the year average minimum temperature is 36°C and average daily minimum is 21°C. Rainfall is generally low with mean annual rainfall ranging from 600mm to 1000mm across the Basin. Much of the rain falls between the months of May to September, while the dry months are October to April (Affordile, 2002).

The geology of Sokoto Basin is very well documented by several authors such as (Jones, 1948; Parker, et al., 1964; Kogbe, 1976; Obaje et al., 2013; and Bonde et al., 2014). According to geologic map of Nigeria (2006), the geology of the study area (Fig. 2) consists of Younger Basalts; Gwandu Formation; Sokoto group consisting of Gamba Formation, Kalambaina Formation and Dange Formation; Rima group consisting of Wuruno Formation, Dukamaje Formation and Taloka Formation; Illo Formation, Gundumi Formation; Pan-African Younger Granitoids and Migmatite-Gneiss Complex.

The sediments of the Sokoto basin were accumulated during different phases of deposition. Overlying the Pre-Cambrian Basement unconformably, is the Illo and Gundumi Formations which are made up of grits and clays, constitute the Pre-Maastrichtian ‘Continental Intercalaire’ of West Africa. They are overlain unconformably by the Maastrichtian Rima Group, consisting of Mudstones and friable Sandstones of Taloka and Wuruno Formations separated by the fossiliferous, calcareous and shaley Dukamaje Formation. The Dange and the Gamba Formations which are mainly shales are separated by the calcareous Kalambaina Formation, which all constitute the Paleocene Sokoto Group. The overlying continental Gwandu Formation forms the Eocene Continental Terminal (Obaje et al., 2013). Figure 3 shows the stratigraphic succession of the sokoto basin.

## **II. Materials And Methods**

### **2.1 Data acquisition and processing**

The high resolution aeromagnetic data that was used for the study consist of sixteen (16) sheets of aeromagnetic maps of total field intensity in half degree sheets obtained from Nigerian Geological Survey Agency (NGSA). The data was acquired by Fugro Airborne Survey Limited, as part of a programme aimed at assisting and promoting mineral exploration in Nigeria using 3X Scintrex CS3 Cesium Vapour Magnetometer with Flight Line Spacing of 500 meter, Flight Line Direction NW-SE, Terrain Clearance 80 meters, Tie Line Spacing 2 kilometres.

The processing of the aeromagnetic data was carried out using various filters that will reveal certain features that will aid the interpretation. Thus the digital data was imported into the computer to produce the total Magnetic intensity map. The Total Magnetic data was further subjected to high resolution filtering techniques such as, polynomial fitting to obtain the regional and the residual maps, upward continuation, Spectral analysis, Curie point depths, etc. All these were carried out using the Oasis montaj 7.0.1 Math lab 10, ArcGIS 10.1

The Polynomial fitting method was used in regional-residual separation to obtain the residual map. In polynomial fitting the regional is matched with mathematical Polynomial of low order to expose the residual features as random errors, and the treatment is based on statistical theory. The observed data are used to compute, usually by least square method, the mathematically described surface given the closest fit to the magnetic field that can be obtained within a specified degree of detail. This surface is considered to be the regional field and the residual is the difference between the magnetic field value thus determined (Udensi, 2001). The simplest approach is to fit a polynomial of first order to the magnetic data over a large area as possible around the zone of interest and to subtract the polynomial surface from the observed surface. If the regional field were a simple inclined plane it will be a first order surface. Thus

$$Z = Ax + By + C \quad (1)$$

The next stage of complexity is the representation of a second order polynomial where,

$$Z = Ax^2 + By^2 + CxyDx + Ey + F \quad (2)$$

The next stage of complexity is another representation of a third order polynomial, etc.

The residual magnetic field of the study area was produced by subtracting the regional field from the total magnetic field using the Polynomial fitting method. The computer program aero-super map was used to generate the coordinates of the total intensity field data values. This super data file, for all the magnetic values was used for production of composite aeromagnetic map of the study area using Oasis Montaj software version 7.0.1 The program was used to derive the residual magnetic values by subtracting values of regional field from the total magnetic field values (Fig.4) to produce the residual magnetic map (Fig. 5).

Upward continuation was used in order to simplify the appearance of regional magnetic anomalies by suppressing the effects due to local features. The proliferation of local magnetic anomalies often obscures the regional features. Upward continuation thus smoothed out these disturbances without impairing the main regional features. The main purpose of upward continuation is to view the magnetic field intensity at a height above flight level so as to eliminate short wavelength anomalies by emphasizing longer ones reflecting regional features. The equation of upward continuation is given by Telford (1990) as;

$$F(x, y, -h) = \frac{h}{2\pi} \iint \frac{f(x,y,0) \partial x \partial y}{(x-x')^2 + (y-y')^2 + h^2)^{3/2}} \quad (3)$$

Where  $F(x', y', -h)$  = total field at a point  $F(x', y', -h)$  above the surface on which  $F(x', y', -0)$  is known.  
 $h$  = continuation height.

This function decays steadily with increasing wave number, attenuating the higher wave number associated with such features and enhances, relatively the anomalies of the deep seated sources because this form continuation effectively smoothens the anomaly, by suppressing the short wave length components. For this study upward continuation was carried out to eliminate local magnetic source, so that the regional sources are enhanced for Curie point-depths calculations. The data was upward continued to 27km (Fig.6). The upward continued data was subjected to spectral analysis, to achieved that the data set was divided into a block of 64 data points, measuring about 15' x 15' which is equal to 27.5km x 27.5km from where the curie point was calculated using Oasis motaj and matlab software.

Curie point depth was estimated in two steps (Bhattacharyya and Leu, 1975 and Okubo et al., 1985): to perform the analysis the first step was to estimate the depth to the centroid ( $Z_o$ ) of the magnetic source from the slope of the longest part of the wave length spectrum.

$$\ln \left[ \frac{p(s)^{1/2}}{/s/} \right] = \ln A - 2\pi/s/Z_o \quad (4)$$

Where  $p(s)$  is the radially average power spectrum of the anomaly,  $/s/$  is the wave number and  $A$  is a constant.

The second step was the estimation of the depth to the top boundary ( $Z_t$ ) of that distribution from the slope of the second longest wave length special segment (Okubo et. al., 1985).

$$\ln p(s)^{1/2} = \ln B - 2\pi/s/Z_t \quad (5)$$

Where  $B$  is the sum of the constant, the basal depth independent of  $/s/$ . Then basal depth ( $Z_b$ ) of the magnetic source was calculated using the equation bellow.

$$Z_b = 2Z_o - Z_t \quad (6)$$

The basal depth ( $Z_b$ ) of the magnetic source in the area is assumed to be the Curie point depth (Bhattacharyya and Leu, 1975 and Okubo et. al., 1985).

Heat flow is the movement of heat (energy) from the interior of earth to the surface. The source of most heat comes from the cooling of the earth's core and the radioactive heat generation in the upper 20 to 40 km of the earth's crust. An average Curie point temperature of 580°C for crustal rocks is recommended (Stacey, 1997 and Nwanko, 2007).

The estimation of heat flow and thermal gradient was calculated using the Fourier's Law with the following formula

$$q = \lambda \left[ \frac{\partial T}{\partial Z} \right] \quad (7)$$

Where  $q$  is the heat flow and  $\lambda$  is the coefficient of thermal conductivity. In this equation it was assumed that the direction of the temperature variation is vertical and the temperature gradient  $\left[ \frac{\partial T}{\partial Z} \right] = \frac{\theta}{Z_b}$  is constant. According to Tanaka et al., (1999), the Curie temperature ( $\theta$ ) is obtained from the Curie point depth ( $Z_b$ )

$$\theta = \left[ \frac{\partial T}{\partial Z} \right] Z_b \quad (8)$$

Provided that there are no heat sources or heat sinks between the earth surface and the Curie point depth, the surface temperature is 0°C and  $\left[ \frac{\partial T}{\partial Z} \right]$  is constant. The Curie temperature depends on the magnetic mineralogy. From equation 7 and equation 8 a relationship was determined between curie depth ( $Z_b$ ) and the heat flow  $q$ , using the following formulae.

$$q = \lambda \left[ \frac{\theta}{Z_b} \right] \quad (9)$$

In the above equation the Curie point is inversely proportional to the heat flow (Tanaka et. al., 1999 and Stamploidset. al., 2005). The geothermal gradient was calculated using equation 8 and a Curie point temperature of 580°C. Also the heat flow ( $q$ ) of the area was calculated using equation 9. In calculating temperature distribution in the crust, thermal conductivity ( $\lambda$ ) is assumed to have a constant value in the range of 2 to 4  $Wm^{-1}C^{-1}$  (Popoola and Ojo, 2010). In this study a thermal conductivity ( $\lambda$ ) of 2.5  $Wm^{-1}C^{-1}$  as average for

igneous rocks was used (Tanaka, et al., 1999, Nwanko, 2007, Popoola and Ojo, 2010 and Abdulsalam, et al., 2011).

### **III. Results And Discussion**

#### **3.1 Results**

The total magnetic intensity map (Fig. 4) of the study area was subdivided into three main sections: The northern part is characterized by low magnetic intensity values indicated by dark- light-blue-green-colour, while the eastern, western as well as the southern parts of the study area are characterized by low magnetic intensity values having dark-light-blue-green-colour dominating the area. The south western and south eastern parts of the study area are dominated by high magnetic intensity values, with pockets of reddish-pink colours disseminated in the northern part. Yellowish-orange-colours accompany the reddish-pink-colours depicting medium magnetic intensity values. The lowest total magnetic intensity value of the study area is 481.4nT and highest value of 633.9nT (Fig.4).

The residual magnetic map, show magnetic anomalies with high magnetic intensity value of 59.6nT and a low magnetic intensity value of -81.2nT. The pink colour anomalies have magnetic intensity ranging from 34.6nT to 59.6nT, which are prominent in the northern and southeastern parts, with pockets in the southwestern part. Red colour anomalies varies from 13.3nT to 30.7nT and are dominant in the northern, central and southwestern parts, with disseminations in the southeastern part. Yellow colour anomalies range from 2.5nT to 11.8nT and occur along the red colour anomalies, dominating the entire map. Green colour anomalies are present in the northern, southeastern, northeastern and southwestern parts, with pockets of small occurrence in the south-south and varies from - 17.2nT to 0.8nT. Blue colour anomalies range from - 81.2nT to - 19.9nT and are the most dominant, occurring in almost every part of the map. The anomalies are trending in the northeast-southwest, northwest-southeast, east-west and north-south direction. Figure 5 shows the residual magnetic map of the Sokoto basin.

The upward continued map, obtained from the residual magnetic map shows a trending of anomalies in the northeast-southwest, northwest-southeast, north-south and east-west direction as in the residual map, with high magnetic intensity of 3.0nT and low magnetic intensity of -4.3nT. The map is characterized with blue, green, yellow, red and pink colour anomalies, similar to the residual magnetic map. Blue colour anomalies ranges from -4.3nT to -1.8nT, green from -1.6nT to -0.2nT, yellow varies from 0.0nT to 0.4nT, red ranges from 0.5nT to 2.3nT and pink from 2.4nT to 3.0nT. A major anomaly of red colour dominates the map, extending from the northern boundary through the central part towards the southwestern part and a second one in the southeastern part, extending from the southern boundary towards the eastern part. The yellow colour anomalies occur alongside the red colour anomalies. While the blue colour anomalies occur in the western part extending from Majiyatudu down to the southern boundary, another blue colour anomaly occur extending diagonally from Zugu in the southeastern part to Dakko, others occur east of Dalijam, north of Tsamiya, southwest of Boto and north of Baraga. Pink colour anomalies occur north of Bangi, west of DarmaGaladima, east of DabanDutse and a major anomaly extending diagonally from southwest to northeast from northeast of Dufua to west of Gamiya. Green colour extends from the eastern boundary diagonally to the southern boundary and from the southern boundary to the north western boundary. Figure 6, shows the Upward continued map of the Sokoto basin.

The graphs of the logarithms of spectral energies against frequencies that were obtained for the various blocks are shown in Figure 7. Two linear segments were drawn from each graph. The depth to the centroid  $Z_o$  of the magnetic source from the slope of the longest part of the wave length spectrum and the depth to the top boundary  $Z_t$  of that distribution from the slope of the second longest wave length segment was calculated and varies from 9.35km to 14.1km and 0.99km to 1.56km respectively. Table 1 shows the summary of the depths ( $Z_o$  and  $Z_t$ ) which was used to compute the Curie point isotherm, geothermal gradient and Heat flow.

The Curie point isotherm map of the study area was obtained using equation 6. The calculated values are presented in Table 1. The Curie point values varies from 17.31km to 26.76km. These values were contoured to obtain the Curie point isotherm map. From the contoured map the area was classified into two divisions. The areas with shallow Curie point depth with values varying from 17.31km to 19.88km covering the entire western part from the northern boundary through Boto, Bangi, DarmaGaladima down to Dakin Gari, SabonGari, Baban Dada, KuramaSuko and Marafa to the southern boundary extending through the central part from Garam, Daji, Lalle, Ganuwa, Gumi through Sokoto town, Maiturare, Dange, Giwa, Kangiwa, Nasarawa, Danpo, Kurus to the eastern boundary. Deeper Curie point depth areas varies from 19.89 km to 26.75 km. these occur in the northeastern part, around northwest of Sokoto town, eastern Wurno, southern Shinaka, around Gwadadi, Dalijam to the eastern boundary and southeastern part of the Sokoto basin around SabonGari, Bulomairimi, Denderis, Tagadi, BirninTudu, Birnin Zuma, South and northeast of Dakko to the eastern boundary down to DabanDutse, Ragam and Daraga down to the southern boundary. Figure 8 shows the Curie point Isotherm map of the Sokoto basin.

The Geothermal gradient map of the study area was obtained using equation 8. The calculated values (Table 1) were used to produce the contoured map. The vertical increase of temperature with depth in the area varies from  $21.67^{\circ}\text{Ckm}^{-1}$  to  $33.50^{\circ}\text{Ckm}^{-1}$ . Two distinct groups of temperature increase with depth were observed on the contoured map. The first group with low temperature increase with depth of  $21.67^{\circ}\text{Ckm}^{-1}$  to  $29.20^{\circ}\text{Ckm}^{-1}$ , occurring in northwest, northeast and southeast of SabonGari; around BuloMaiturare, Denderis, Tagadi, BirninTudu, Birnin Zuma, northeast and south of dakko to the eastern boundary down to Daraga, DabanDutse, Ragam, Mahuta to the southern boundary and in the northern boundary through the southeastern and southern part of DarmaGaladima, Shinaka, around Wurno, Sokoto town, northern and eastern Barsawa, Ilela, Dange, Kangiwa, to the northeastern boundary. The second group, with high temperature increase with depth of  $29.21^{\circ}\text{Ckm}^{-1}$  to  $33.50^{\circ}\text{Ckm}^{-1}$ , dominates the entire map from the western boundary through the central part to the eastern boundary, occurring through Boto, Bamgi down to Dakin Gari, Baban Dada, SabonGari, KuramaSuko, Marafa, Gumi, northern Dakko and from DarmaGaladima, through Bunkari, southern and western Barsawa, Ilela, southern Dange, Kangiwa, Nasarawa and around Dampo to the east. It was clearly observed that areas with high Curie point depth have low geothermal gradient while areas with low Curie point depth have high geothermal gradient. Figure 9 shows the geothermal gradient map of the Sokoto basin.

The heat flow values of the area were obtained using equation 9 (Table 1). The values were contoured to obtain the Heat flow map. The heat flow varies from  $54.18\text{mWm}^{-2}$  to  $83.64\text{mWm}^{-2}$ . From the contoured map of the heat flow, the area was classified into low and high heat flow areas. Low heat flow areas have values varying from  $54.18\text{mWm}^{-2}$  to  $70.59\text{mWm}^{-2}$ , which occur in the southeastern and northeastern parts from Mahuta, BuloMairimi, Denderis, Dakko to the east through Anka, Doka, Banaga, Daraga, to Ragam and DabanDutse to the south and northeastern Gandi, Gwadadi, eastern Wurno, Southern Shinaka to the northeast. These correspond with areas of high Curie point depth but with low geothermal gradient. High heat flow areas have values varying from  $70.60\text{mWm}^{-2}$  to  $83.64\text{mWm}^{-2}$ , which occur from the eastern boundary through the central part to the western boundary from the northern boundary down to the southern boundary, cutting across from Boto, Bamgi, DarmaGaladima to Dakko Gumi, Denderis, BuloMairimi, to Mahuta, Marafa, KuramaSuko, Daban Dada, SabonGari and Dakin Gari to the South and from RafinKalgo, BirninKebbi town, Ungwan Dole, Kamsu, Lema to Gandi, Kangiwa, Nasarawa and Dampo to the east. This area correspond with areas of low Curie point depths but with high geothermal gradient. Figure 10 shows the Heat flow map of the Sokoto basin.

### 3.2 Discussion

The Curie point depth reflect the average local temperatures beneath each block, at which magnetic elements loss their magnetic properties. It was observed that the depth of Curie point (Fig.8) in the study area varies from 17.31km to 26.75km. Shallow Curie depths ranging from 17.31km to 19.88km were observed at almost the entire area with exception of a portion in the northwest of Sokoto town, east of Wurno, east of Denderis, east of Gumi and south of Dakko. Shallow anomalies of 17.31km to 18.16km were observed at southeast of Masaari with elongation of east to west with approximately length of 19km and a width of approximately 18km, northeast of Giwa with elongation of east to west with length of approximately 20km and a width of approximately 14km, a circular anomaly northwest of Dakko with an approximate diameter of 7km, a circular anomaly northeast of Tokwacho approximately 7km in diameter and a circular anomaly southwest of Dampo with an approximate diameter of 13km. Also a shallow anomaly with curie depth of 18.17km to 19.02km was observed east of Jakuka with an elongation of east to west with length of 25km and a width of 23km.

Deeper Curie depth values varies from 19.89 km to 26.75 km were observed in the southeastern part of the study area around east of Denderis, east of Gumi and south of Dakko. In the northeastern part northwest of Sokoto town and east of Wurno. A circular anomaly of 19.89 km to 20.74 km was observed at the northwest of Sokoto town with a diameter of approximately 17km; an anomaly with curie depth of 20.75 km to 24.18 km with an elongation of east to west with length of 32 km and a width of 23km was observed in the northeast of Gwadadi; a circular anomaly with curie depth of 25.05km to 25.90km was observed in the northwest of Donko with an approximate diameter of 12km; anomalies were also observed northeast of Doka with curie depth of 25.91km to 26.75km with elongation of north to south with approximate length of 19km and a width of 9km, an anomaly with curie depth of 25.91km to 26.75km southwest of Gwashi with elongation of north to south, length of approximately 11 km and a width of 9km and an anomaly with curie depth of 25.91km to 26.75km South of Ragam, around Bamaga and Daraga with elongation of east west, length of approximately 65 km and a width of 22km.

The general trend of the curie depth in the study area shows that curie depth increases from west to east. That is curie depth isotherm decreases from 26.75km to 17.31km from east to west in the study area, indicating that the crust is thinning towards the west. Shallow curie isotherm depths are ascribed to where the

crust is thin while deeper Curie isotherm depths of 25.91km to 26.75km could be as a result of thick crust isostatic compensation in the region (Kasidi and Nur, 2012)

Comparing the result of the Curie depth with geothermal studies carried out in the Sokoto basin and adjoining Nupe basin of Nigeria, it was observed that the research carried out by Suleiman (2012) shows a Curie point depth of 5.14km to 9.80km. Also Ofor and Udensi (2014), showed that the Curie depth of the Sokoto basin varies from 11.36km to 22.30km. However Nwonkoet al., (2007), carried out a research over the Nupe basin North Central Nigeria, showed that the Curie point depth varies from 12km to 13km.

The variation of Curie depths between the study area of the Sokoto basin (17.31km to 26.75km) and the Nupe basin (12km to 13km), could be attributed to geological conditions which greatly affect the Curie point of a particular area (Nwonkoet al., 2007). The result of this research shows disparity with that of Suleiman (2012) and agree to some extent with that of Ofor and Udensi (2014). The disparity could be as a result of the difference in the resolution of the data used. The fore mentioned researchers used analog data while the present research make use of high resolution digital data. Considering the topography (Fig. 1) and geology of the area, it is clear that the topography of the area increases in height from west to east, low topography areas have low to moderate Curie depths while deeper Curie depths of 26.75km are peculiar to the Basement rocks (Fig. 2).

Geothermal gradient is the increase of temperature with depth. In this study the geothermal gradient (Fig.9) of the study area varies between  $21.67^{\circ}\text{Ckm}^{-1}$  and  $33.51^{\circ}\text{Ckm}^{-1}$ . Low values of geothermal gradient varying from  $21.67^{\circ}\text{Ckm}^{-1}$  to  $29.20^{\circ}\text{Ckm}^{-1}$  were observed at the southeast of the geothermal gradient map, east of Denderis, east of Gumi, south of Dakko and in the northeast of the geothermal gradient map, northwest of Sokoto town, east of Wurno and south of Shinaka. Anomaly of low geothermal gradient of  $21.67^{\circ}\text{Ckm}^{-1}$  to  $23.82^{\circ}\text{Ckm}^{-1}$  was observed northwest of Donko with an elongation of northwest to southeast with an approximate length of 20km and a width of 15km; a circular anomaly with geothermal gradient of  $21.67^{\circ}\text{Ckm}^{-1}$  to  $22.74^{\circ}\text{Ckm}^{-1}$  west of Karun with an approximate diameter of 5km, also a major area of low geothermal gradient of  $21.67^{\circ}\text{Ckm}^{-1}$  to  $22.74^{\circ}\text{Ckm}^{-1}$  was observed south of Gwashi with an elongation of east to west, length of approximately 67km and an approximate width of 45km; a circular anomaly with geothermal gradient of  $27.06$  to  $28.12^{\circ}\text{Ckm}^{-1}$  occur northwest of Sokoto town with an approximate diameter of 15km; an anomaly with elongation of east to west was also observed north of Dalijam, with a length of approximately 25km and a width of approximately 22km with geothermal gradient of  $22.75^{\circ}\text{Ckm}^{-1}$  to  $25.97^{\circ}\text{Ckm}^{-1}$ .

High geothermal gradient values of  $29.21^{\circ}\text{Ckm}^{-1}$  to  $33.50^{\circ}\text{Ckm}^{-1}$  occur almost in the entire map apart from the low areas in the northeast and southeast. Anomalies with high geothermal gradient of  $32.44^{\circ}\text{Ckm}^{-1}$  to  $33.50^{\circ}\text{Ckm}^{-1}$  were observed south of BirninKebbi with an elongation of north to south, length of approximately 89km and approximate width of 29km; anomaly with an elongation of east to west, with length of approximately 43km and a width of approximately 8km north of Boto; a circular anomaly west of Bunkari with approximate diameter of 22km; a circular anomaly northwest of Gamiya with approximate diameter of 5km; a circular anomaly with diameter of approximately 5km southwest of Maiturare and a circular anomaly southwest of Dampo with approximate diameter of 2.5km. Other circular anomalies with geothermal gradient of  $32.38^{\circ}\text{Ckm}^{-1}$  to  $32.43^{\circ}\text{Ckm}^{-1}$  were observed southeast of Ilella with an approximate diameter of 13km, an anomaly east of Kurus with diameter of 18 km and an anomaly south of Walu with an approximate diameter of 8km.

The pattern of the geothermal gradient in the area increases from east to west unlike the Curie point depth which increases in depth from west to east. This further confirm the characteristic thinning of the crust towards the western part of the study area with the increasing thermal gradient to the western part. Geothermal gradient is the increase of temperature with depth. That is the out flow of heat from the earth interior to the surface of the earth, while Curie point is the temperature at which magnetic elements loses their magnetic properties and become paramagnetic. It can be established that Curie point and geothermal gradient are inversely proportional.

Relating the result of the geothermal gradient with other works in the Sokoto basin and nearby basins, Ofor and Udensi (2014), obtained thermal values ranging from  $26.18^{\circ}\text{Ckm}^{-1}$  to  $44.62^{\circ}\text{Ckm}^{-1}$  in the Sokoto basin, while Suleiman (2012), obtained thermal values of  $30.61^{\circ}\text{Ckm}^{-1}$  to  $58.37^{\circ}\text{Ckm}^{-1}$ . The calculated thermal depth of the study area is similar to what has been estimated by Ofor and Udensi (2014) and that of the Nupe Basin ( $19^{\circ}\text{Ckm}^{-1}$  to  $46^{\circ}\text{Ckm}^{-1}$ ) Nwankwo, et al., (2007).

The calculated heat flow (Fig.10) of the study area varies between  $54.18\text{mWm}^{-2}$  to  $83.64\text{mWm}^{-2}$ . Low heat flow values varies from  $54.18\text{mWm}^{-2}$  to  $70.59\text{mWm}^{-2}$  covering the southeastern part of east of Bulomairimi, east of Denderis, east of Gumi and south of Dakko. Various anomalies of low heat flow were observed in the area. These include a circular anomaly of heat flow of  $54.18\text{mWm}^{-2}$  to  $59.50\text{mWm}^{-2}$  with a width of approximately 12km northwest of Donko; a circular anomaly of  $54.18\text{mWm}^{-2}$  to  $56.85\text{mWm}^{-2}$  west of Kerun with a width of approximately 5km; an anomaly of  $54.18\text{mWm}^{-2}$  to  $59.85\text{mWm}^{-2}$  south of Gwashi with an elongation of east to west, with a length of approximately 50km and width of approximately 48km. Also in the northeastern part, an area of low heat flow occur in the northwest of Sokoto town, east of Wurno and south of

Shinaka. An anomaly of  $56.86\text{mWm}^{-2}$  to  $64.89\text{mWm}^{-2}$  is observed in this area with an elongation of east to west, with length of approximately 29km and width of approximately 22km and a circular anomaly with heat flow of  $67.58\text{mWm}^{-2}$  to  $70.59\text{mWm}^{-2}$  northwest of Sokoto town with diameter of approximately 16km.

High heat flow ranges from  $70.60\text{mWm}^{-2}$  to  $83.64\text{mWm}^{-2}$  covering the entire map with exception of low heat flow areas of the southeast and northeast. The anomalies of the area include: an anomaly  $80.98\text{mWm}^{-2}$  to  $83.64\text{mWm}^{-2}$ , with an elongation of north to south, length of approximately 77km and width of about 29km south of BirninKebbi; a circular anomaly with heat flow value of  $78.30\text{mWm}^{-2}$  to  $80.97\text{mWm}^{-2}$  with a diameter of about 13km southeast of Ilella; a circular anomaly of heat flow value of  $78.30$  to  $80.97\text{mWm}^{-2}$  south of Kurus with diameter of about 14km; a circular anomaly of heat flow value of  $80.98\text{mWm}^{-2}$  to  $83.64\text{mWm}^{-2}$  with diameter of approximately 2.5km southeast of Argungu; a circular anomaly of heat flow of  $80.98\text{mWm}^{-2}$  to  $83.64\text{mWm}^{-2}$  southwest of Maiturare with diameter of about 6km; a circular anomaly of heat flow value of  $80.98\text{mWm}^{-2}$  to  $83.64\text{mWm}^{-2}$  northwest of Gamiya with an approximate diameter of 6.2km; a circular anomaly with heat flow value of  $80.98\text{mWm}^{-2}$  to  $83.64\text{mWm}^{-2}$  southwest of Dampo with diameter of about 3.3km; a circular anomaly with heat flow of  $80.98\text{mWm}^{-2}$  to  $83.64\text{mWm}^{-2}$  west of Bunkari with an approximate diameter of 21km; an anomaly of heat flow of  $80.98\text{mWm}^{-2}$  to  $83.64\text{mWm}^{-2}$  north of Boto with an elongation of east to west, length of approximately 40km and width of approximately 13km and an anomaly with heat flow of  $72.94\text{mWm}^{-2}$  to  $75.61\text{mWm}^{-2}$  east of Lalle with an elongation of northwest to southeast, length of approximately 22km and width of approximately 20km.

The average heat flow in a thermally normal continental region is about  $60\text{mWm}^{-2}$ , values between  $80\text{mWm}^{-2}$  to  $100\text{mWm}^{-2}$  are good geothermal sources. While values greater than  $100\text{mWm}^{-2}$  is an indication of anomalous geothermal condition (Jessop et al., 1976). These also corresponds with the areas of high geothermal gradient and low Curie point depth. This shows that heat flow is inversely proportional to Curie point. The area with high heat flow as observed from the heat flow map could serve as a geothermal source of energy. The study shows that all the heat flow values are within the recommended (normal) range, no anomalous value that was recorded in this study.

Currie point depth, geothermal gradient and heat flow are dependent on geological conditions (Ofor and Udensi, 2014). Generally high heat flow correspond to volcanic and metamorphic regions, since these two units have high heat conductivities. Also heat flow is affected by tectonically active regions (Tanaka, et al., 1999). Geothermal energy also do occur in areas where Basement rocks that have relatively normal heat flow are covered by thick blanket of thermally insulated sediments. This therefore means that the areas with high heat flow in the study area may be inferred as areas where thick blanket of thermally insulated sediments cover Basement rocks since there is no evidence of volcanic activity in the study area.

Geothermal studies deals with the study of heat of the Earth, implying that geothermal gradient is the rate at which the earth's temperature increases with depth. Meaning that heat is flowing from the hot earth's interior to the surface. Two basic sources of heat are known in nature, these are magma and radioactive sources. Others include impact and compression of the earth in the release of meteorites, heat released from electromagnetic effects of the earth's magnetic field, heat released during tidal force on the earth as it spins along its axis and rotates since land cannot flow like water, it compresses and distorts thereby generates heat (Adedapo et al., 2013).

The understanding of the heat flow of the earth aid in the knowledge of the thermal structure of the earth crust, thus determines the modes of deformation, ductile and brittle deformation zones, regional heat flow variations, seismicity, subsidence and uplift patterns and maturity of organic matter in sedimentary basins (Dolmaz, et al., 2005). The thermal crustal structure in the Sokoto basin base on the result of Currie point depth, shows that the crust is thinning in areas of shallow Curie depth of 17.31km to 18.16km. This could be the reason of the trend of high heat flow and increase of geothermal gradient in such areas of curie depth.

## **IV. Conclusion And Recommendation**

### **4.1 Conclusion**

The following conclusion can be drawn from this work:

- (1) The Curie point isotherm deduce from the study, indicate that the crust is thinning in areas of shallow Curie point depth in the western part of the study area.
- (2) The geothermal gradient shows that the area is characterized into low and high temperature zones. Low temperature zones could not allow the thermal maturation of sediments, high temperature zones could result into thermal maturation of sediments and hence probable oil generation.
- (3) Areas with high heat flow were investigated and delineated and therefore these are the prospective areas for geothermal energy, which could be used in generating electricity to argument the epileptic power supply that is being experienced in the country; it can also be used for domestic, industrial and agricultural purposes.

## 4.2 Recommendation

The study area if given much attention, will boost the economic growth of the country based on the potentials for geothermal sources revealed by this study. Therefor the following recommendation are made:

- (1) The use of other geophysical methods such as seismic, well logging in drilled boreholes should be encouraged
- (2) A detailed geophysical, geochemical and basic geology of the area needs to be carried out for effective interpretation of geothermal potentials in the area.

## Acknowledgementt

The authoris grateful to the Nigerian Geological Survey Agency (NGSA), for releasing the High Resolution Digital Aeromagnetic data at a subsidized rate and Adamawa State University, Mubi Nigeria, for granting the author a study fellowship.

## References

- [1]. Abdulsalam, N.N., Nasir, M.A. and Likason, K.O. Identification of Linear Features Using Continuation Filters over KotonKarfi Area from Aeromagnetic Data. *World Rural Observation*: Vol. 3(1),2011, Pp. 1-8
- [2]. Adedapo, J.O., Kurowska, E., Schoeneich, K. and Ikpokonte, A. E. Geothermal Gradient of the Niger Delta from Recent Studies. *International Journal of Scientific and Engineering Research*: Vol. 4, Issue 111,2013, Pp.39-45.
- [3]. Affodile, M.E. Ground water study and development in Nigeria: 2<sup>nd</sup> Edition; Mecon Geology and Eng., Services Ltd., Jos Nigeria,2002, 453p.
- [4]. Bhattacharryya, B. K. and Leu, L. K. Spectral analysis of gravity and magnetic anomalies due to two dimensional structures: *Geophysics*, Vol. 40,1975, Pp. 993 – 10313.
- [5]. Blackwell, D.; Negraru., P.; Richards, M. Assessmentof the enhance geothermal system resource base of theUnited States, *Nat. Res. Res.*, 15(4):2006,Pp. 283-308.
- [6]. Bonde, D.S., Udensi, E.E. and Rai, J.K. Spectral Depth Analysis of Sokoto Basin. *Journal of Applied Physics*: Vol. 6, Issue I,2014, Pp. 15-21.
- [7]. DiPippio, R. *Geothermal power plants: Principles, applications and case studies*. Butterworth einemann:Elsevier, Oxford, England.2005.
- [8]. Dolmaz, N.M., Ustaomer, T., Hisarli, M.Z., and Aibay, N. Curie point depth variation to infer thermal structure of the crust at the African-Eurasian convergence zone, SW Turkey. *Earth Planets Space*, Vol. 51,2005.Pp. 373 – 383.
- [9]. Jones, B. *Sedimentary Rocks of the Sokoto Province*. Bulletin of the Geological Survey of Nigeria, Kaduna 18,1948, 79p.
- [10]. Kasidi and Nur, A. Curie depth isotherm deduced from spectral analysis of Magnetic data over sarti and environs of North-Eastern Nigeria: *Scholarly Journals of Biotechnology* Vol. 1(3), 2012, Pp. 49-56.
- [11]. igerian Geological Survey Agency, NGSA. Geological Map of Latitude 11<sup>o</sup>30' - 13<sup>o</sup>30'and Longitude 4<sup>o</sup>00' and 6<sup>o</sup>00', 2006.
- [12]. Nigeria Geological Survey Agency, NGSA. High Resolution Aeromagnetic Data, (16 Sheets), Latitude 11<sup>o</sup>.30' – 13<sup>o</sup>.30' and Longitude 4<sup>o</sup>.00' - 6<sup>o</sup>.00', 2010.
- [13]. Nigeria Geological Survey Agency, NGSA. Topographic Map of Latitude 11<sup>o</sup>.30' – 13<sup>o</sup>.30' and Longitude 4<sup>o</sup>.00' - 6<sup>o</sup>.00', 2006.
- [14]. Nwanko, L.I. Spectral evaluation of aeromagnetic anomaly map for geothermal exploration in part of Nupe basin, west central Nigeria. Ph.D Thesis University of Ilorin.2007.
- [15]. Oasis montaj7.0.1 QX Geosoft Inc. Queens Quay terminal, 207 Queens Quay west suit 810, P.O.BOX 131 Ontario Canada.
- [16]. Obaje, G.N., Aduku, M and Yusuf, L. The Sokoto Basin of Northwestern Nigeria: A Preliminary Assessment of the Hydrocarbon Prospectivity. *Petroleum Technology Development Journal*: Vol. 3, No. 2,2013, Pp. 66-80.
- [17]. Ofor, N.P. and Udensi, E.E. Determination of the Heat flow in the Sokoto Basin, Nigeria Using Spectral Analysis of Aeromagnetic Data. *Journal of Natural Science Research*: Vol. 4, No. 6,2014, Pp. 83-93.
- [18]. Parker, D.H., Fargher, Carter, M. N., Turner, O. C. Geological Map of Nigeria Series 1:250,000. Sheet Nos, 1, 2, 3, 6, 7 and 8.1964.
- [19]. Popoola, O.I. and Ojo, A.E. Effects of poor conductor on continental crust heat flow parameters. *Pacific journal of science and Technology*. 11(1),2010,Pp. 483-501.
- [20]. Salem, A., Ushijima, K., Elsirafi, A. and Mizunaga, H. Spectral Analysis of Aeromagnetic data for Geothermal Reconnaissance of Quseir Area, Northern Red Sea Egypt. *Proceedings World geothermal Congress Kyushu-Tohoku, Japan, 2000*, Pp.1669-1674.
- [21]. Stacey, F.D. *Physics of the earth*. John Wiley and Sons, New York, 1997, 414p.
- [22]. Stampolidis, A., Kane, I., Tsokas, G.N. & Tsourlo, P. Curie point depths of Albania inferred from ground total magnetic data. *Surveys in Geophysics*, Vol. 26, 2005, Pp. 461 – 481.
- [23]. Suleiman, T. Investigation of the geothermal source potential across Kebbi State, Nigeria using aeromagnetic data. Unpublished M.Sc. thesis.2012.
- [24]. Tanaka, A., Okubo, Y. and Matsubayashi, O. Curie point depth base on spectrum analysis of the magnetic anomaly data in east and Southeast Asia. *Tectonophysics*, 306, 1999, Pp. 461 – 470.
- [25]. Telford, W.M., Geldart, L.P., and Sheriff, R.E. *Applied Geophysics* (2<sup>nd</sup> Edition) Cambridge University Press.1990.

[26]. Udensi, E.E. Interpretation of Total Magnetic Field over the Nupe Basin and the Surrounding Basement Complex, Using Aeromagnetic Data. Unpublished Ph.D. Thesis submitted to Ahmadu Bello University, Zaria.2001.

Table 1: Calculated Curie point depth, geothermal gradient and heat flow of the study area.

Block Depth to the centroid (Z<sub>c</sub>) Depth to the top boundary (Z<sub>b</sub>)(θ) Curie point depth (q) Geothermal gradient Heat flow

1	9.78	1.28	18.28	31.73	79.32	
2	9.56		1.43		17.69	32.77
81.97						
3	9.52		1.32		17.72	32.73
81.83						
4	9.89		1.44		18.34	31.63
79.06						
5	9.73		1.48		17.98	32.26
80.65						
6	9.94		1.39	18.49	31.37	78.42
7	10.23		1.30		19.16	30.27
75.68						
8	10.43		1.34	19.52	29.71	74.28
9	9.64		1.46		17.82	32.55
81.37						
10	9.71		1.50	17.92	32.37	80.92
11	9.83		1.21		18.45	31.44
78.59						
12	9.35		1.37		17.31	33.51
83.77						
13	10.82		1.16	20.48	28.32	70.80
14	10.31		1.24	19.38	29.93	74.82
15	12.45	1.10		23.80	24.37	60.92
16	11.97	1.40		22.54	25.73	64.33
17	9.63	1.35		19.91	29.13	72.83
18	9.72	1.52		17.92	32.37	80.92
19	9.64	1.52		17.92	32.37	80.92
20	9.59		1.20	17.98	32.26	80.65
21	10.54	1.43	19.65	29.52	73.79	
22	10.57		1.46	19.68	29.47	73.68
23	10.23		1.16	19.30	30.05	75.13
24	10.78		1.49	20.07	28.90	72.25
25	9.67	1.14		18.20	31.87	79.67
26	9.62		1.23	18.01	32.20	80.51
27	9.73		1.56	17.90	32.40	81.01
28	9.88	1.34		18.42	31.49	78.72
29	9.45	1.07		17.83	32.53	81.32
30	9.62	1.41	17.83	32.53	81.32	
31	9.67		1.49	17.85	32.49	81.23
32	9.83		1.46	18.20	31.87	79.67
33	9.38		1.08	17.62	32.92	82.29
34	9.64		1.35	17.93	32.35	80.87
35	9.98		1.03	18.93	30.64	76.60
36	10.53		1.28	19.78	29.32	73.31
37	9.76		1.43	18.09	32.06	80.15
38	9.80		1.21	18.39	31.54	78.85
39	9.74		1.53	17.95	32.31	80.78
40	10.96		1.44	20.48	28.32	70.80
41	9.64		1.03	18.25	31.78	79.45
42	9.63		1.39	17.87	33.39	83.48

43	9.72	1.44	18.00	32.22	80.56
44	9.87	1.50	18.24	31.80	79.50
45	10.45	1.20	19.70	29.44	73.60
46	11.38	1.29	21.47	27.01	67.54
47	12.79	1.45	24.13	24.04	60.09
48	13.12	1.27	24.97	23.23	58.07
49	9.51	1.02	18.00	32.22	80.56
50	9.53	1.47	17.59	32.97	82.43
51	9.79	1.15	18.43	31.47	78.68
52	11.36	1.45	21.27	27.27	68.17
53	13.52	1.39	25.65	22.61	56.53
54	13.54	1.45	25.63	22.63	56.57
55	13.81	1.52	26.10	22.22	55.56
56	13.89	1.47	26.31	22.05	55.13
57	9.46	1.13	17.75	32.68	81.69
58	9.74	1.13	18.35	31.61	79.02
59	9.83	0.99	18.66	31.08	77.70
60	9.89	1.08	18.70	31.02	77.55
61	13.11	1.37	24.85	23.34	70.85
62	13.67	1.20	26.14	22.19	55.48
63	13.93	1.20	26.66	21.76	54.40
64	14.10	1.44	26.76	21.67	54.18

Figures

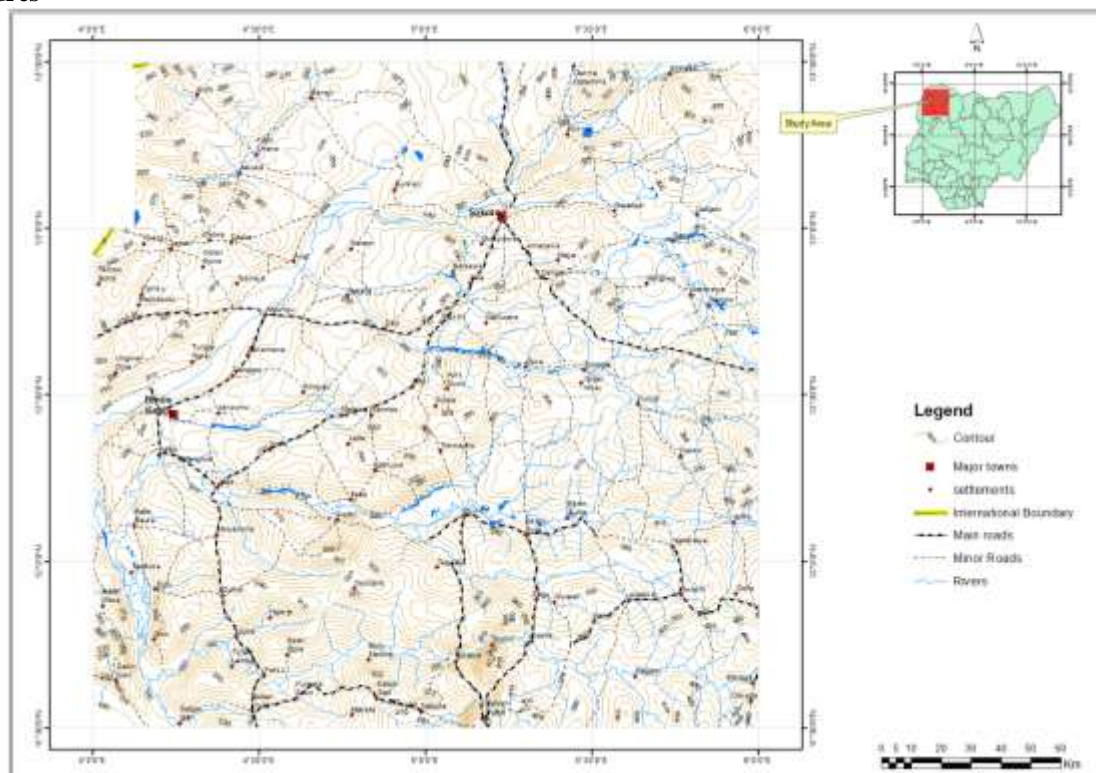


Figure 1: Topographic Map of the Study Area [Analyzed From Digital Elevation Model (DEM) 2006]

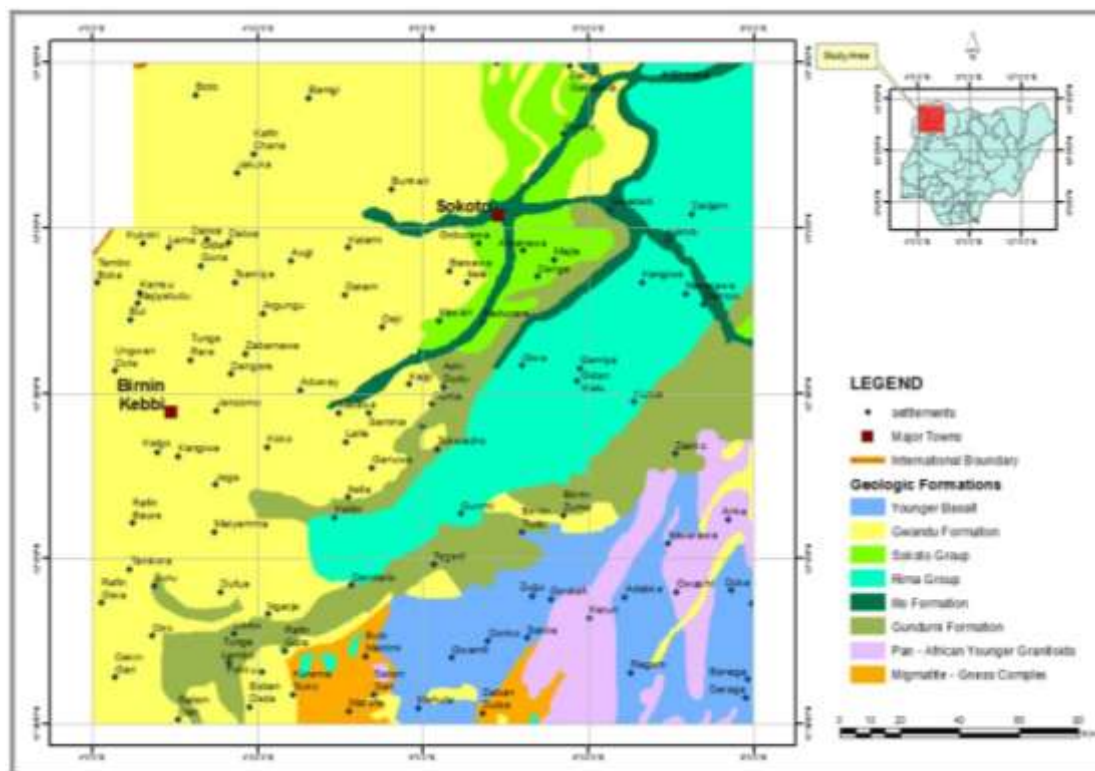


Figure 2: Geologic Map of the Study Area (After Nigerian Geologic Survey Agency, 2006)

Eocene	Sokoto Group	Gwandu Formation	Continental	Continental Terminal
		Gamba Formation	Marine	
		Kalambaina Formation	Marine	
Paleocene	Sokoto Group	Dange Formation	Marine	
		Wurno Formation	Continental	
		Dukamaje Formation	Marine	
Maastrichtian	Rima Group	Taloka Formation	Continental	
		Gundumi-Ilo Formation	Continental	Continental Intercalaire
<b>Basement</b>				

Figure 3: Stratigraphic Succession in the Nigerian Sector of the Illummeden (Sokoto) Basin (Modified after Obaje, et. al., 2013).

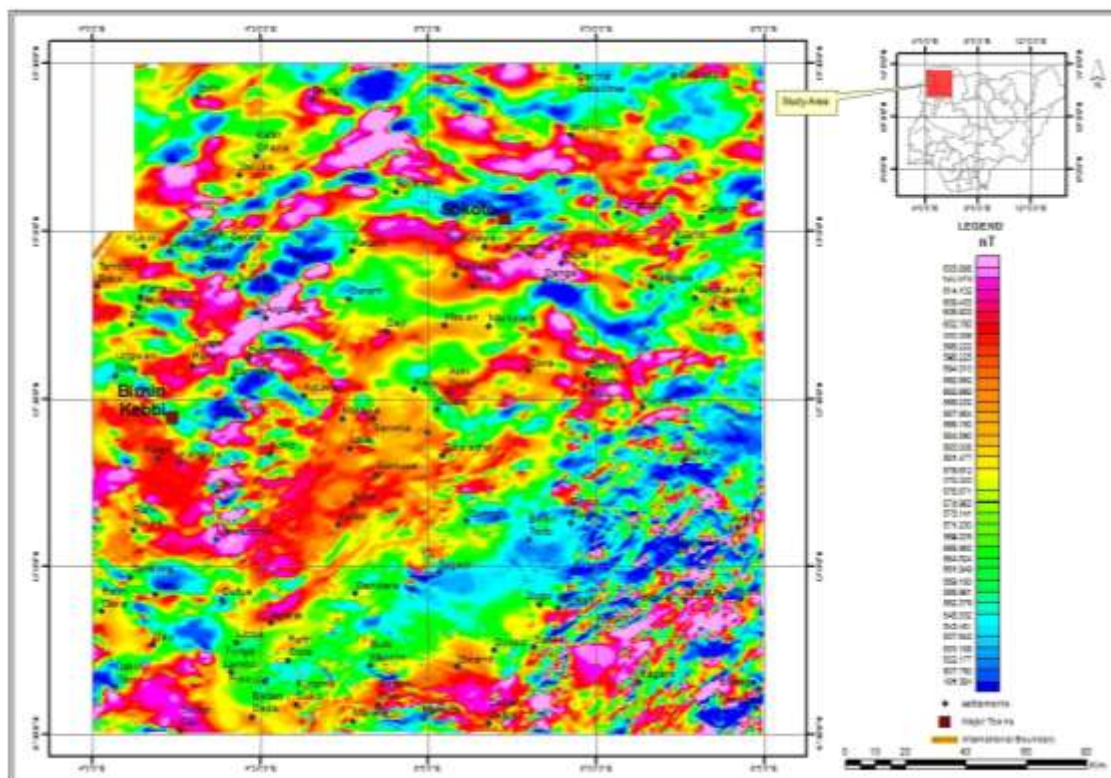


Figure 4: Total Magnetic Intensity Map of the Study Area.

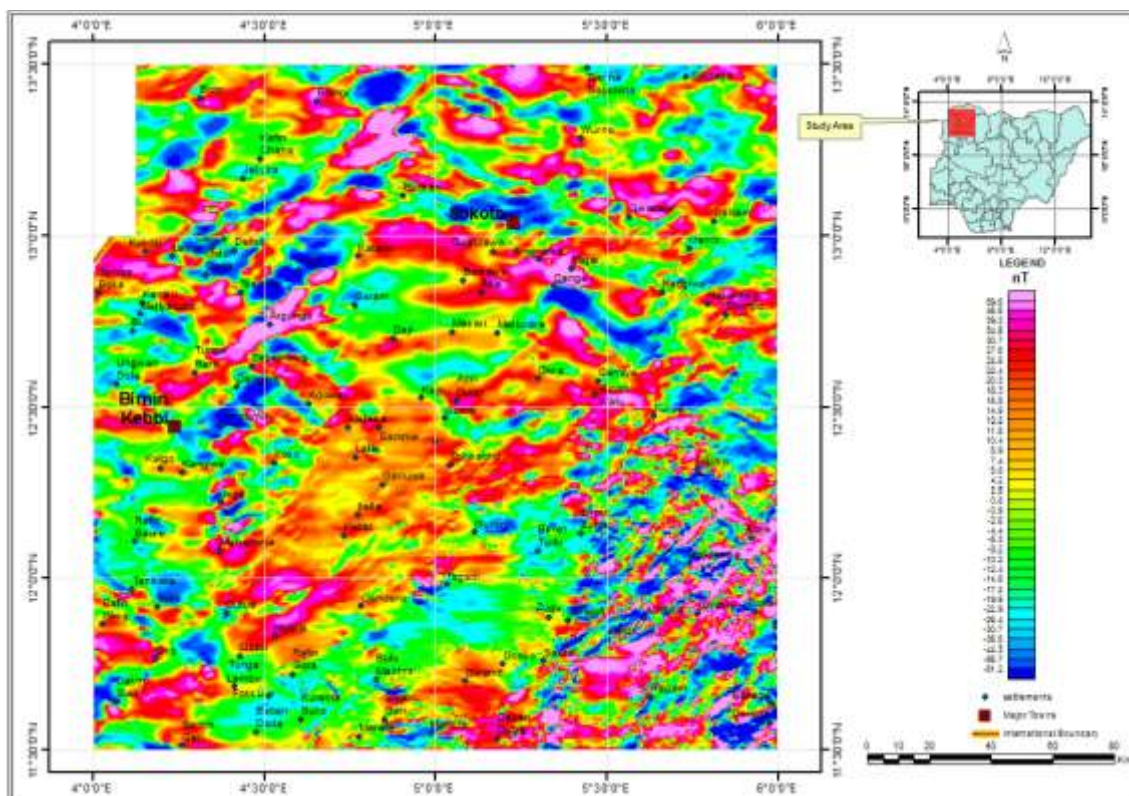


Figure 5: Residual Magnetic Intensity Map of the Study Area.

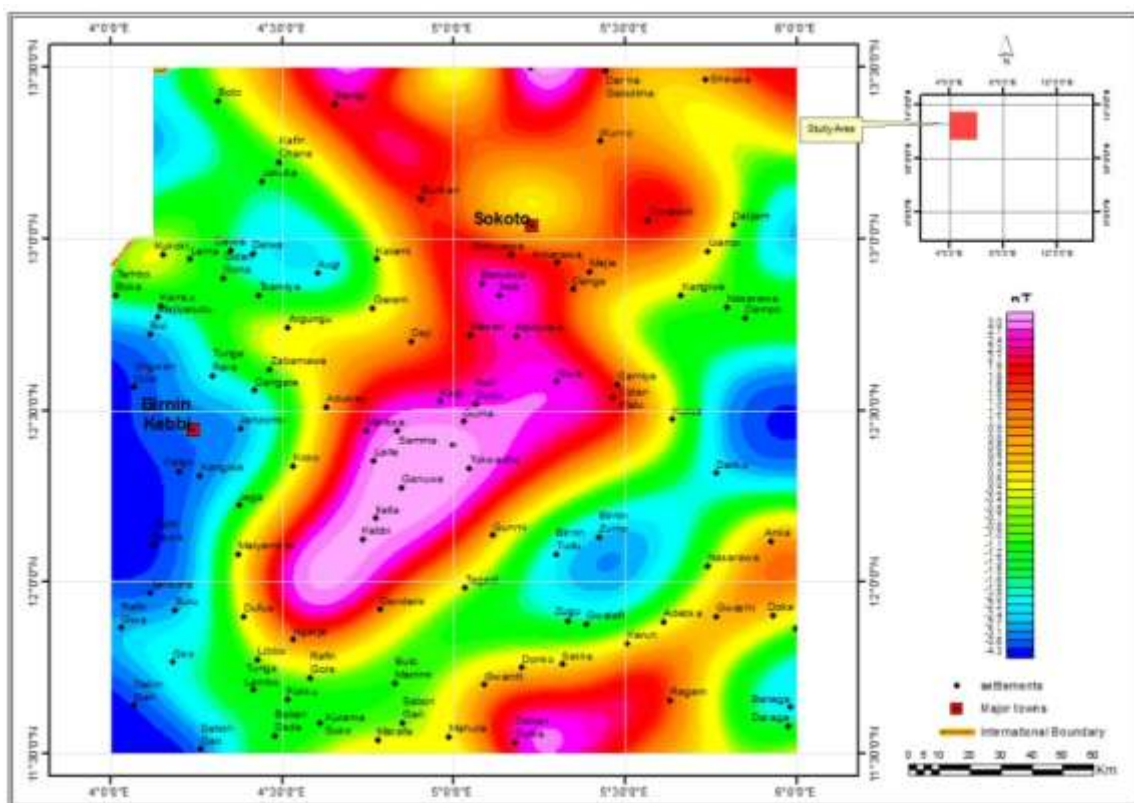


Figure 6: Residual Magnetic Map of the Study Area Upward Continued to 27 km.

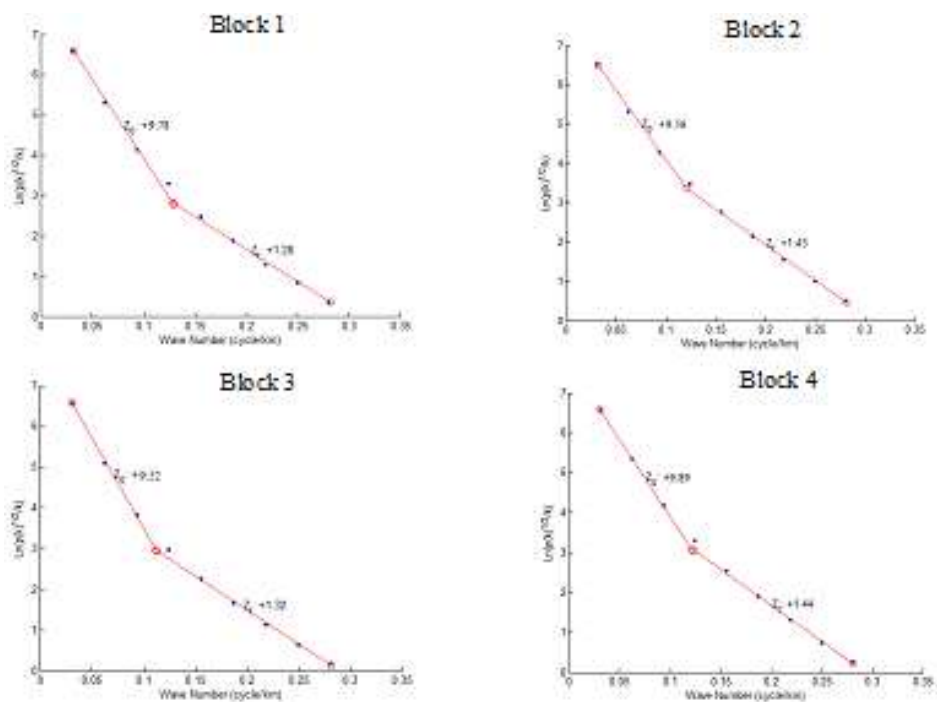


Figure 7: Examples of Spectra Blocks Obtained from the Study Area.

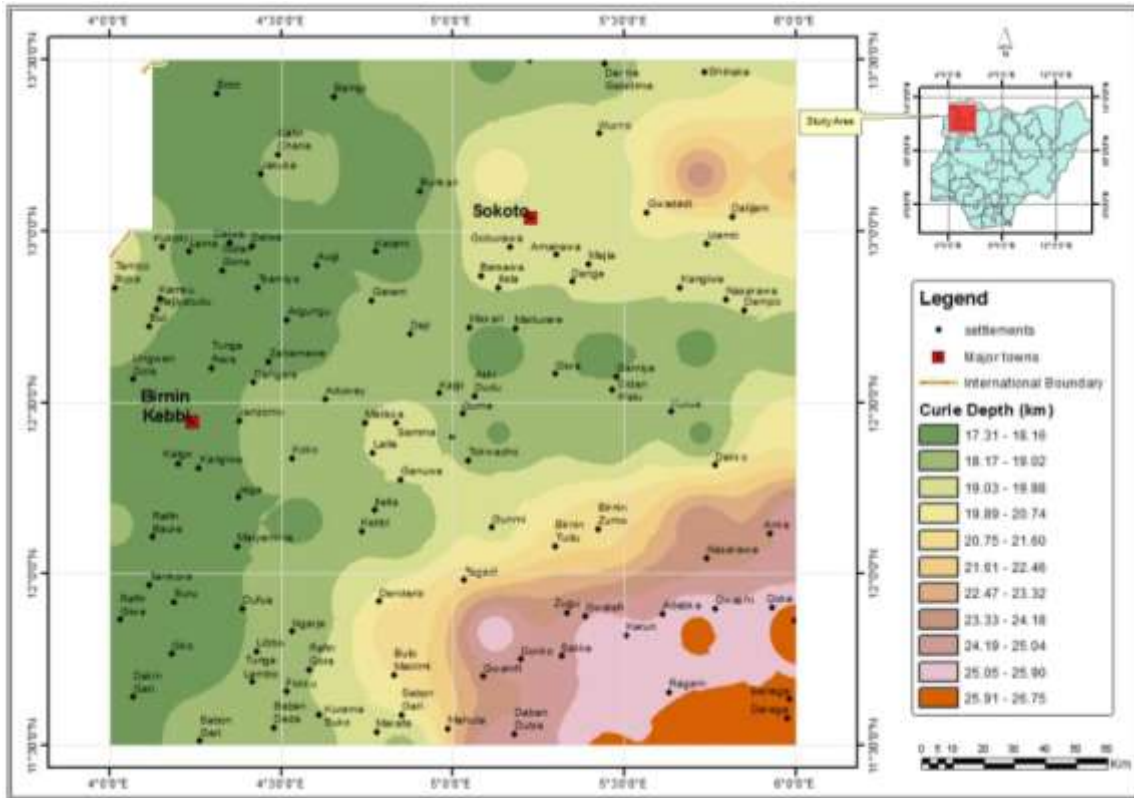


Figure 8: Curie point depth Map of the Study Area.

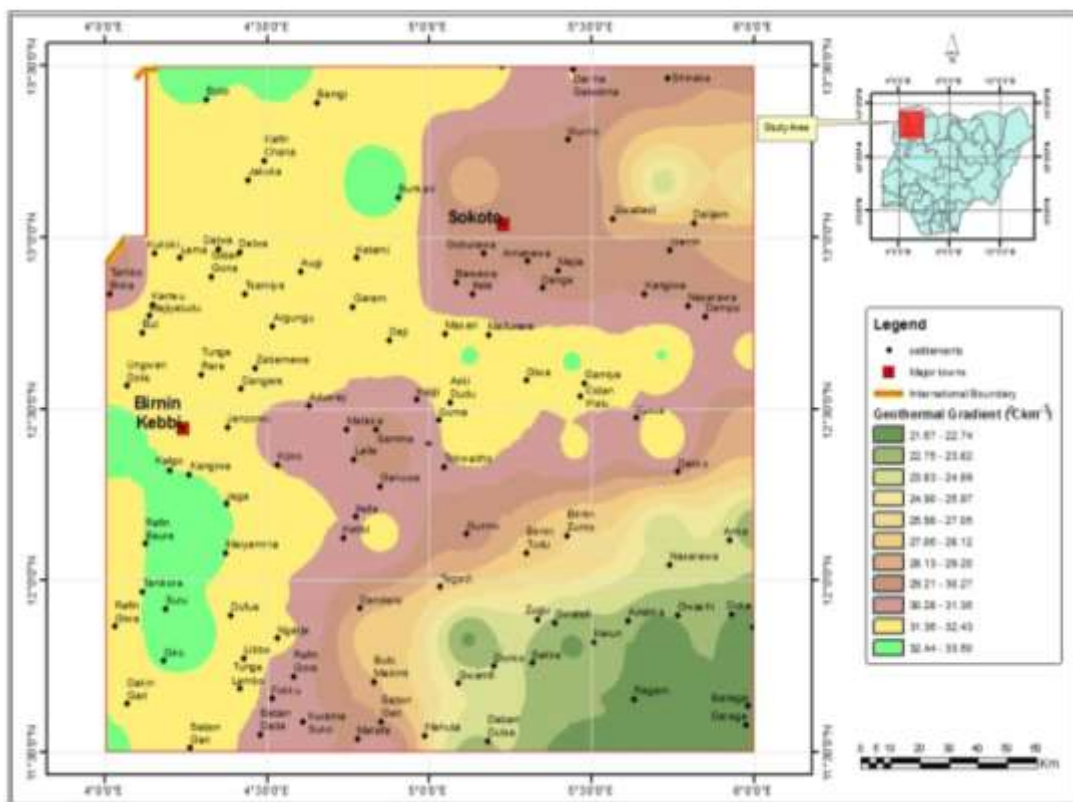


Figure 9: Geothermal gradient Map of the Study Area.

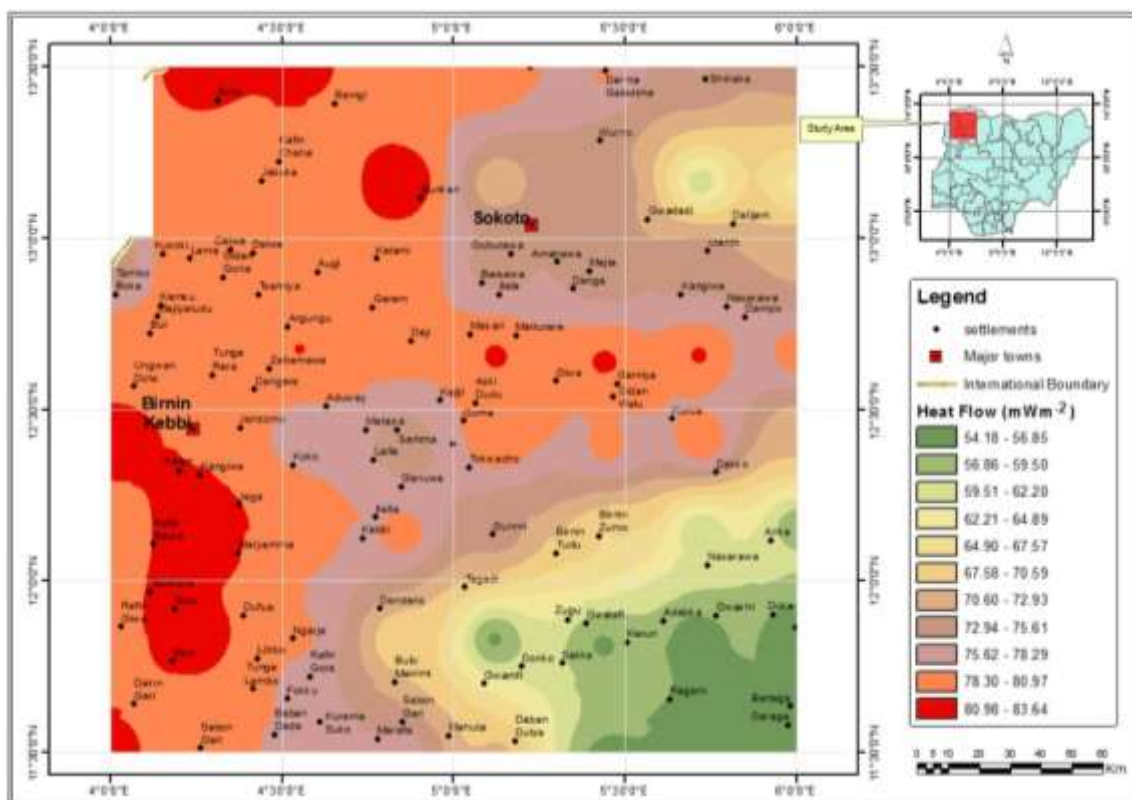


Figure 10: Heat Flow Map of the Study Area.

Kamureyina Ezekiel" Geothermal Study Over Sokoto Basin Northwestern, Nigeria" International Journal of Engineering Science Invention (IJESI), Vol. 08, No. 05, 2019, PP 34-48